SOLID PHASE ADHESION OF TUNGSTEN AND SILVER

by

William M. Saunders

B.Sc. - University of Alberta, 1965

ABSTRACT OF DISSERTATION

Submitted in partial fulfillment of the requirements for the degree

of Master of Science in Solid State Science and Technology in the

Graduate School of Syracuse University, August 1967.

Approved _____

Date _____

ABSTRACT

Solid phase adhesion of the bulk immiscible metals silver and tungsten
has been investigated, using the method of Johnson and Keller. The
strength of the junction approximated the tensile strength of silver.
A model for metallic adhesion was suggested, which predicts an ad-
hesion strength which approaches the tensile strength of the weaker
metal in the couple between all pairs of metals.

ACKNOWLEDGEMENTS

TABLE OF CONTENTS

LIST OF TABLES AND ILLUSTRATIONS

INTRODUCTION

When two solid metallic surfaces are brought into intimate contact, certain physical interactions occur along the interface which result in an attractive force between the bodies. This phenomenon is often referred to as metallic adhesion or cold welding. It is an important consideration in the design of space craft components, since the lack of atmospheric gases in the space environment (cf. Table 1) increases the probability of the occurrence of metallic adhesion (2). Keller (1) has shown that the process is also an important factor in the mechanism of friction. Many investigations of the factors influencing adhesion have been carried out, but few have yielded any fundamental knowledge of the phenomenon. Many adhesion studies (3,4,5) have been carried out in air, which causes severe surface contamination; however, Johnson and Keller (2) have established that surface contamination is the major barrier to adhesion. Extreme deformation along the interface can disperse these contaminants, and, as a consequence, a number of ductile metals have been cold-welded in air by the application of high compressive stresses (3,4,5). However, these experiments give little insight into the basic phenomenon since the degree of contamination and deformation involved in the experiment is not readily measurable.

Of the investigations that have been carried out in vacuum low enough to prevent rapid surface contamination, i.e. at least 10^{-9} Torr (cf. Table 1), many still involve obvious surface contamination and require gross deformation to permit adhesion. For example, one common procedure is to fracture a tensile specimen in vacuum, bring the pieces back together in compression, and then refracture the cold-welded sample (6,7,8,9). The compressive stress necessary to rejoin the pieces is typically greater

TABLE I

ALTITUDE (IN 100,000 FT.)

APOGEE OF SPUTNIK I ──── ──── SEA LEVEL

Altitude scale: 60 50 40 30 20 15 10 7 5 4 3 2.5 2 1.5 1 0.5 0

PRESSURE (TORR)

10^{-12} 10^{-11} 10^{-10} 10^{-9} 10^{-8} 10^{-7} 10^{-6} 10^{-5} 10^{-4} 10^{-3} 10^{-2} 10^{-1} 1 10 10^2 10^3

DENSITY (MOLECULES/CM^3 AT 25°C)

10^5 10^6 10^7 10^8 10^9 10^{10} 10^{11} 10^{12} 10^{13} 10^{14} 10^{15} 10^{16} 10^{17} 10^{18} 10^{19}

MEAN FREE PATH (IN. AT 25°C)

10^{-6} 10^{-5} 10^{-4} 10^{-3} 10^{-2} 10^{-1} 1 10 10^2 10^3

MEAN FREE PATH (MILES AT 25°C)

10^4 10^3 10^2 10 1 10^{-1}

IMPINGEMENT RATE (MOLECULES/CM^2/SEC AT 25°C)

10^9 10^{10} 10^{11} 10^{12} 10^{13} 10^{14} 10^{15} 10^{16} 10^{17} 10^{18} 10^{19} 10^{20} 10^{21} 10^{22} 10^{23}

TIME TO FORM MONOLAYER (SEC AT 25°C)

10^2 10 1 10^{-1} 10^{-2} 10^{-3} 10^{-4} 10^{-5} 10^{-6} 10^{-7} 10^{-8} 10^{-9}

(HR. AT 25°C)

10^2 10 1

than the yield stress for the particular material, which implies that the fracture surfaces must be highly deformed before significant adhesion occurs. During such a test, contamination may occur from sources other than the ambient gases, such as gas filled voids within the metal, surface diffusion of impurities from the sides of the specimen onto the freshly formed surface, or from diffusion of impurities from the bulk of the sample to the new surface. Indeed, many investigators using this technique have reported a violent pressure rise when the specimen was fractured.

Hordon and his co-workers (10) have produced voluminous adhesion data from experiments in which the surfaces were presumably cleaned by brushing them with a stainless steel brush in ultra-high vacuum. This technique suffers from the fact that mass transport of brush material (or surface contaminants on the brush) to the specimens undoubtedly occurs as well as surface roughening, heating and work hardening. The surfaces in these experiments were therefore in some unknown complex state, preventing the observation of fundamental phenomena.

In 1960, Keller (2,11,12,13) initiated a program to investigate the fundamental aspects of metallic adhesion. It was apparent that such an investigation would require samples with atomically pure, well-defined surfaces, which could be brought together with nearly zero loading to keep deformation at a minimum. An apparatus was developed which approximated these conditions well. (See Experimental section of this thesis.)

Early exploratory investigations by Keller (13) and others (4) which did not attempt to measure the force of attraction indicated that adhesion occurred between metals which were mutually soluble in the bulk, and did not occur between bulk insoluble pairs. However, more recent and more sophisticated investigations in which actual force measurements were taken

established that this is doubtful (2). The insoluble couple silver (Ag)-tungsten (W) was selected for study in this investigation for the following reasons:

(1)   ease of preparing atomically clean surfaces for both metals,

(2)   to further investigate the solubility criterion for metallic adhesion, and

(3)   to further investigate the contact resistance of dissimilar couples, since Johnson et al (2) reported anomalously high contact resistances between dissimilar metals.

THEORY

Atomic Nature of The Adhesion Force

The exact nature of the adhesion force across the interface between two metals is not known; however, it is generally accepted that the force is closely related to those forces which bind the atoms of a bulk metal together, i.e. the metallic bond. This may be illustrated intuitively by considering the following ideal experiment. A perfect metallic crystal is cleaved in a perfect vacuum at $0°K$, and the two pieces are brought back together into a forceless contact in exactly the same configuration. The resulting interface within the crystal should be indistinguishable from other similar planes throughout the crystal. In fact, we should again have a perfect single crystal, held together by the metallic bond. Such an experiment could not be performed, even at acceptably low (but finite) temperature and pressure since the metal cannot always be cleaved. Further, it is impossible to bring the halves back together with exactly the same relative position. It is also most difficult to prevent contamination of the clean surfaces, and to achieve a forceless contact. Even so, it seems logical to assume that if the ideal conditions were approximated, the adhesive force will be closely related to the metallic bond.

In this investigation, there were two important deviations from the ideal experiment:

(1) Adhesion was achieved by gently bringing two atomically clean wires into contact. Since the samples were polycrystalline, it was impossible to achieve a crystallographic match when the surfaces were brought together. However, the regions of intimate contact were probably in a state somewhat like a grain boundary since the surfaces were carefully cleaned and lightly

loaded. Therefore, the ideal conditions were approximated.

(2)   Dissimilar metals were used. Such a junction may be analyzed using solution theory if the interface is considered to be a region of finite thickness with a concentration gradient (this is discussed in detail in the "Results and Discussion" section of this thesis). The atoms in such an interface should be held together by the metallic bond.

In summary, despite the deviations from ideality in this experiment, it is probable that the adhesion forces observed were very similar to the metallic bond across a grain boundary.

Effect of Surface Contamination

Johnson and Keller (2) indicated that surface contamination is the major barrier to adhesion for soft metals (2), and probably for hard metals (12). Furthermore, they demonstrated that there are two classes of contaminant barriers to adhesion; one class could be removed simply by reducing the gas pressure around the sample, and the other could only be removed by rigorous argon ion cleaning of the surfaces. Stable films, such as those formed under long exposure to atmospheric conditions, constitute the latter class.

Energy Barrier to Adhesion

Erdmann-Jesnitzer (14) and Semenov (15) proposed the existence of an energy barrier to adhesion which consisted of the work required to align the surface atoms to form an interfacial bond. Johnson and Keller (2,12) showed that this barrier, if it exists, is of minor importance in the phenomenon of metallic adhesion.

Effect of Elastic Relief Forces

The failure by elastic forces of interfacial atomic bonds

(on unloading) was postulated by Bowden, Tabor et al (16,17), largely in connection with metallic friction studies. Such a model may apply to contaminated surfaces; however, in the case of atomically clean surfaces, elastic relief forces do not significantly contribute to the weakening of the interfacial bond (1,11).

Effect of Mutual Solubility

As discussed in the Introduction, early experiments seemed to indicate that insoluble metals do not adhere (13,4). However, Johnson and Keller (2) have shown conclusively that the insoluble silver-nickel couple adheres. There is also evidence that the insoluble copper-tantalum and iron-silver couples adhere (10), although it is less conclusive than the evidence presented by Johnson and Keller for silver-nickel. Thus, when the present investigation began, it was suspected that mutual solubility is not a criterion for the existence of metallic adhesion.

Estimation of Bond Strengths

The most important datum obtained from an adhesion experiment is the stress at which the adhesion couple breaks. The force to break the junction is relatively simple to measure, but the true area of metal-metal contact is extremely difficult to obtain. This is because the surfaces of the sample are never perfectly smooth, particularly after cleaning by argon ion bombardment. Therefore, even for atomically clean surfaces in contact, if the loading is light, there will be regions that are not in contact within the apparent contact area. If the surfaces are contaminated the problem is even more complex since there will be contaminants dispersed over the contact area that may or may not prevent intimate contact.

At present, there is no accurate method to measure true contact area. However, there are two methods available which give contact area to a first approximation.

(1)   Contact Resistance Method

As an approximation, consider one circular contact region between two members of the same metal with clean surfaces. Holm (18) has shown that the radius of the contact region (a) can be estimated from the equation:

$$R_c = \frac{\rho}{2a} \qquad (1)$$

where R_c is the contact, or constriction, resistance, and ρ is the specific resistivity of the metal. The term contact resistance was coined at a time when it was believed that the metallic contact surface itself accounted for the observed resistance. Actually, the observed resistance is a constriction resistance which is the consequence of the current flow being constricted through small conducting spots (18). For a dissimilar metal couple, (1) becomes

$$R_c = \frac{\rho_1}{4a} + \frac{\rho_2}{4a} \qquad (2)$$

where ρ_1 and ρ_2 are the specific resistivities of the two metals.

It should be noted that these formulae apply only to clean surfaces. If a contaminant film is present, a corrective term must be added due to the thickness and resistivity of this film (18).

Recently, Greenwood (19) has re-evaluated Equation (1) for surfaces with asperities and demonstrated that R_c must be given by the equation:

$$R_c = \rho \left(\frac{1}{\pi n^2} \sum_{i \neq j} \sum \frac{1}{r_{ij}} + \sum_i \frac{1}{2a_i} \right)$$

where ρ is the metal conductivity

          n   is the number of metal junctions formed

         r_{ij} is the distance between junction "i" and junction "j"

         a_i is the radius of junction "i"

However, such an equation could not be used in the present investigation, since n, r_{ij} and a_i are most difficult to measure.

Johnson et al found that contact areas calculated using Equation (1) gave anomalously high values of junction strengths for couples loaded below 30 mg. They therefore rejected it in favor of Hertz' method, which is derived from mechanical considerations.

(2)   <u>Hertz Method</u>

Figure (1) shows a plot of the average pressure, P_m, vs load for an idealized couple of perfect geometry as discussed by Tabor (20). Section OA is the elastically deformed region, BC the plastic region and AB a transition zone. In the elastic region OA, Hertz (21) has shown that for crossed cylinders (the configuration used in this investigation) the radius of the contact zone is given by:

$$a = \left[\frac{3}{4} W \left(\frac{1-\sigma_1^2}{E_1} + \frac{1-\sigma_2^2}{E_2} \right) \left(\frac{1}{r_1} + \frac{1}{r_2} \right)^{-1} \right]^{1/3} \tag{3}$$

where   a   =   radius of contact zone

         W   =   load

         σ =   Poisson's ratio

         E   =   Young's modulus of elasticity

         r   =   radius of curvature of couple members

Section BC of the P_m versus load plot may be approximated (18) by the hardness of the material, i.e.

$$P_m = H$$

The initiation of plastic deformation occurs at a load W_A (20) when

$$P_m = 1.1y$$

where y is the yield strength of the material.

With the substitution of the data for silver in subscript 1 of Equation (3), the value for a of the tungsten-silver couple can be shown to be:

$$a = \left[\frac{3}{4} W \left(\frac{1 - (0.37)^2}{7 \times 10^8} + \frac{1 - (0.30)^2}{35.1 \times 10^8} \right) \left(\frac{1}{.050} + \frac{1}{.038} \right)^{-1} \right]^{1/3}$$

or

$$a = \left[2.42 \times 10^{-11} W \right]^{1/3} \tag{5}$$

where the values for the mechanical parameters have been taken from Holm (18) and the Metals Handbook (22). This equation will only be acceptable below the load W_B above which the silver yields by plastic deformation alone. At this load we have from Equation (4):

$$\frac{W_B}{A} = H \, ,$$

where

$$A = \text{contact area}$$

or

$$W_B = H\pi a^2 \tag{6}$$

The hardness (V.P.N.) of the silver specimen was found to be $\frac{k_g}{mm^2}$ at 200 gm load (2). We can also substitute Equation (5) into Equation (6) for a. Then Equation (6) becomes:

$$W_B = 48.3 \times 10^5 \pi \left[2.42 \times 10^{-11} \, W_B \right]^{2/3}$$

$$W_B = \left[48.3 \times 10^5 \pi \right]^3 \left[2.42 \times 10^{-11} \right]^2$$

$$W_B = 2.1 \text{ gm}$$

The loading range in this investigation was 0.5 to 7.5 gm. Since the Hertz equation was derived assuming an elastic interaction and since W_B (the load at which the silver rod will deform in a completely plastic manner) is about 2 gm, we can only apply the Hertz equation for loads less than 2 gm. However, Johnson et al (2) found that Holm's equation (Equation (1)) gave satisfactory results for heavier loads (e.g. > 0.5 gm for Ag-Ag). Therefore, for loads < 1.5 gm, Equation (3), the Hertz equation will be applied, and for loads > 1.5 gm, Equation (1), Holm's equation will be used.

It should be emphasized that both of these equations assume perfectly smooth specimen surfaces. In reality there are asperities on the surface that will deform plastically (although the load will be carried in the bulk material by predominately elastic deformation) (23). It is clear, then, that the contact area of the adhesion couple can only be crudely estimated. Equations (1) and (3) are only fair approximations, but they are used in this analysis because they are the only acceptable equations available.
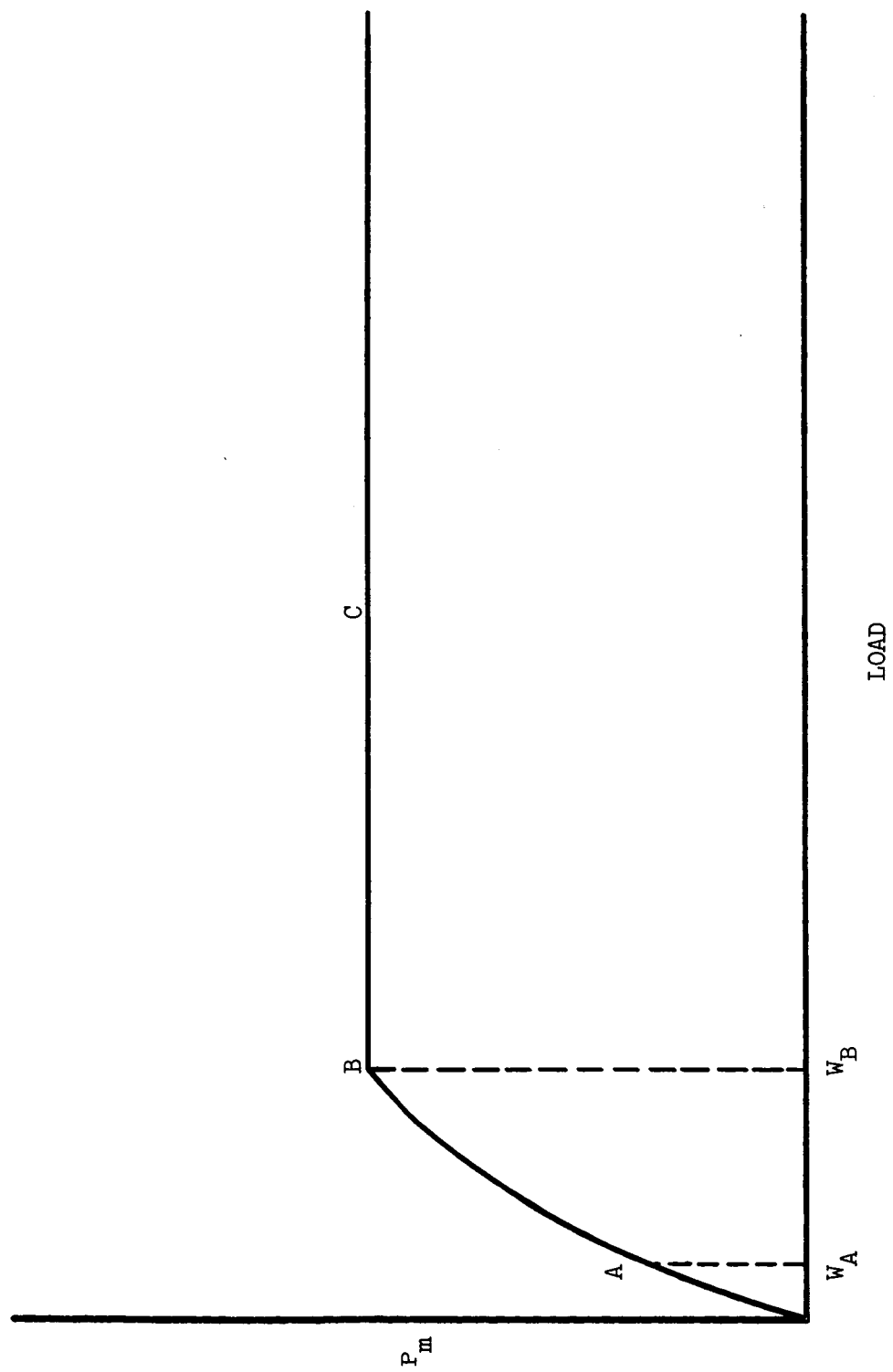
FIGURE 1 PRESSURE VS. LOAD.

EXPERIMENTAL

The adhesion cell and pumping system were designed to allow the measurement of the contact resistance and adhesion strength between two metal samples as a function of contact force, with varying degrees of surface contamination. The system consisted of a 40 x 300 mm pyrex adhesion cell (A) attached through a 1" ultra-high vacuum valve (H) to the vacuum system, as shown in Figure 2. The adhesion cell, valve, and first liquid nitrogen trap were baked out during each experiment at pressures below 10^{-6} Torr at a temperature of 450°C for at least 15 hours. After bake-out, the degassing of the titanium sorption pump (G), and the cooling of the first liquid nitrogen trap, the pressure in the adhesion cell was usually 2×10^{-10} Torr, as measured by the NRC Redhead gauge (D) mounted adjacent to the specimens. The titanium sorption pump consisted of a helix of 0.010" titanium wire closely wrapped over 0.015" tungsten wire which, in turn, was formed into a 1/8" helix.

The torsion beam and adhesion samples are shown in Figure 3. Figure 4 indicates specific details of the beam support. The beam pivot consisted of a .006 in. tungsten wire mounted on a support fixed in a "Conflat" flange which was remote from all electrical leads. This method of supporting the beam is an improvement to the method developed by Johnson et al (2,12), since the leads to each sample and to the electron bombardment filaments were well separated from each other. This eliminated the possibility of electrical breakdowns during the high voltage processes of argon ion cleaning and electron beam annealing of the samples.

The beam was constructed of two pieces of tubing joined with a stainless steel connector which served to support the beam on the pivot wire. The alumina tubing supporting the sample had two holes through which
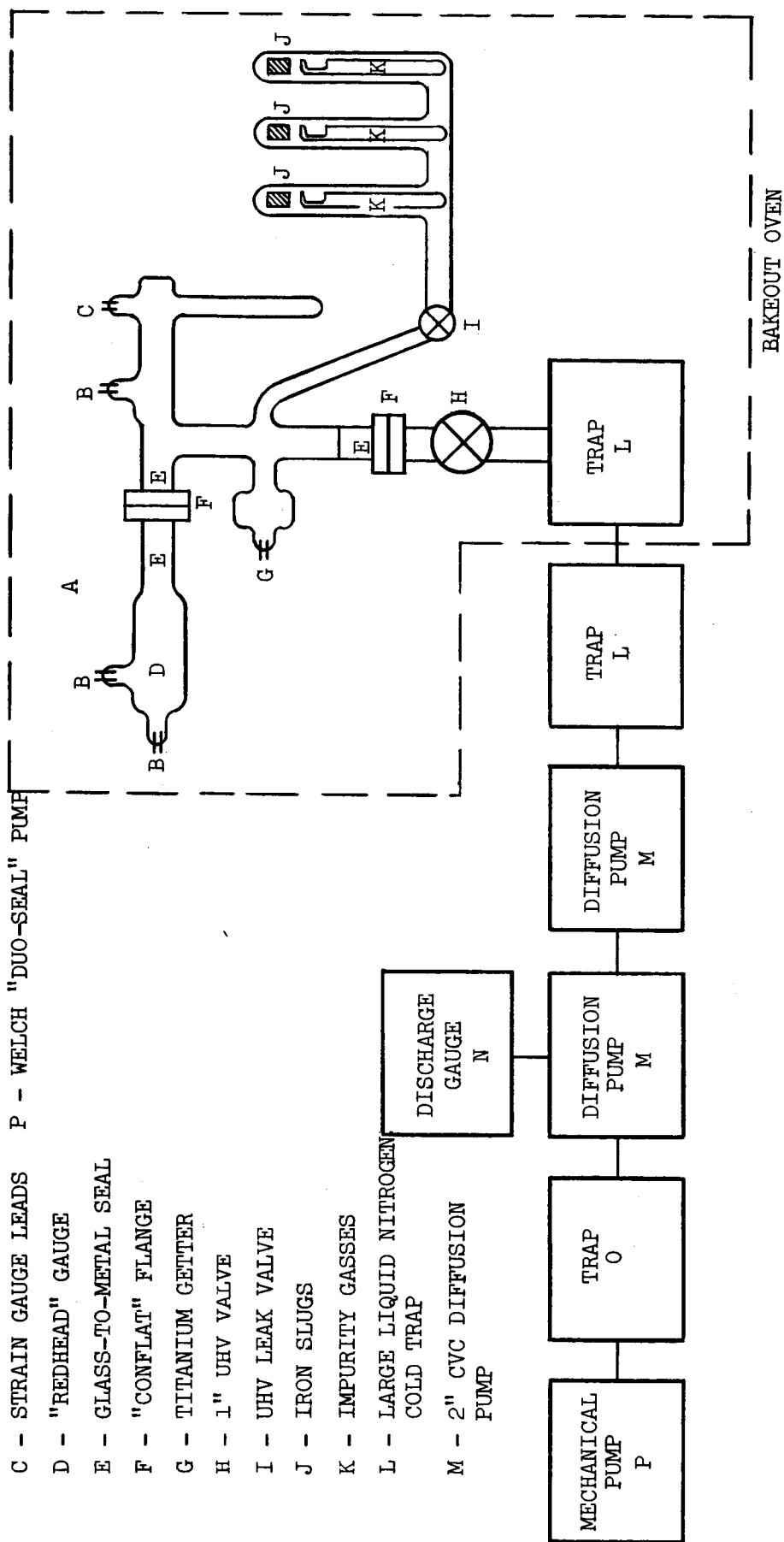
A – ADHESION CELL
B – SAMPLE LEADS
C – STRAIN GAUGE LEADS
D – "REDHEAD" GAUGE
E – GLASS–TO–METAL SEAL
F – "CONFLAT" FLANGE
G – TITANIUM GETTER
H – 1" UHV VALVE
I – UHV LEAK VALVE
J – IRON SLUGS
K – IMPURITY GASSES
L – LARGE LIQUID NITROGEN COLD TRAP
M – 2" CVC DIFFUSION PUMP

N – CVC DISCHARGE GAUGE
O – SMALL LIQUID NITROGEN COLD TRAP
P – WELCH "DUO–SEAL" PUMP

FIGURE 2 VACUUM SYSTEM.

A – SAMPLE LEADS   M – MAGNET
B – SAMPLE HOLDERS   N – STRAIN GAUGE
C – SAMPLES   O – SOLENOID
D – FILAMENT
E – REDHEAD GAUGE
F – GLASS–TO–METAL SEAL
G – CONFLAT FLANGE
H – TITANIUM GETTER
I – IMPURITY GAS SOURCE
J – VACUUM SYSTEM
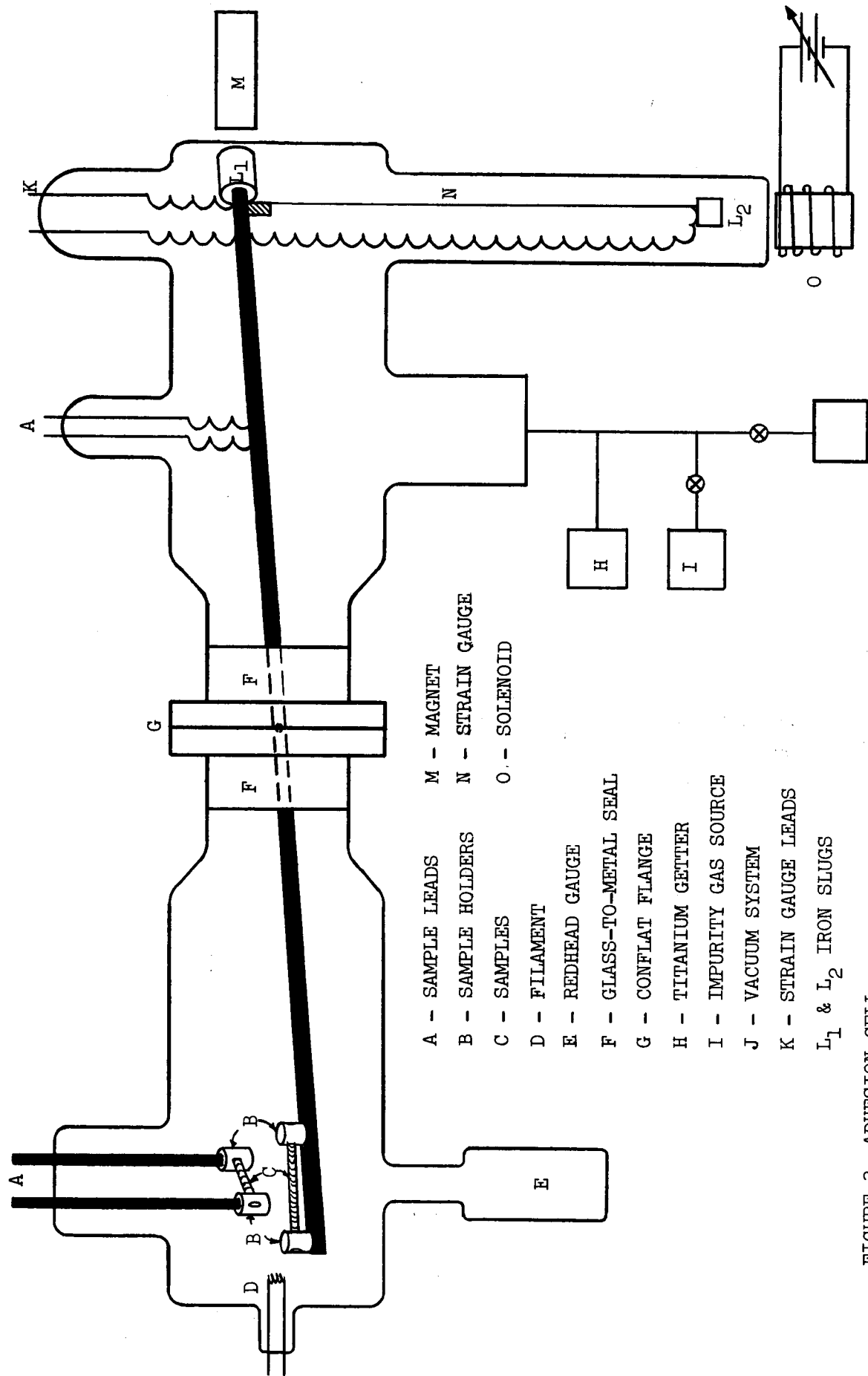K – STRAIN GAUGE LEADS
L_1 & L_2 IRON SLUGS

FIGURE 3   ADHESION CELL

A - "CONFLAT" FLANGE   E - BOLT HOLE

B - GASKET SEAT   F - SET SCREWS
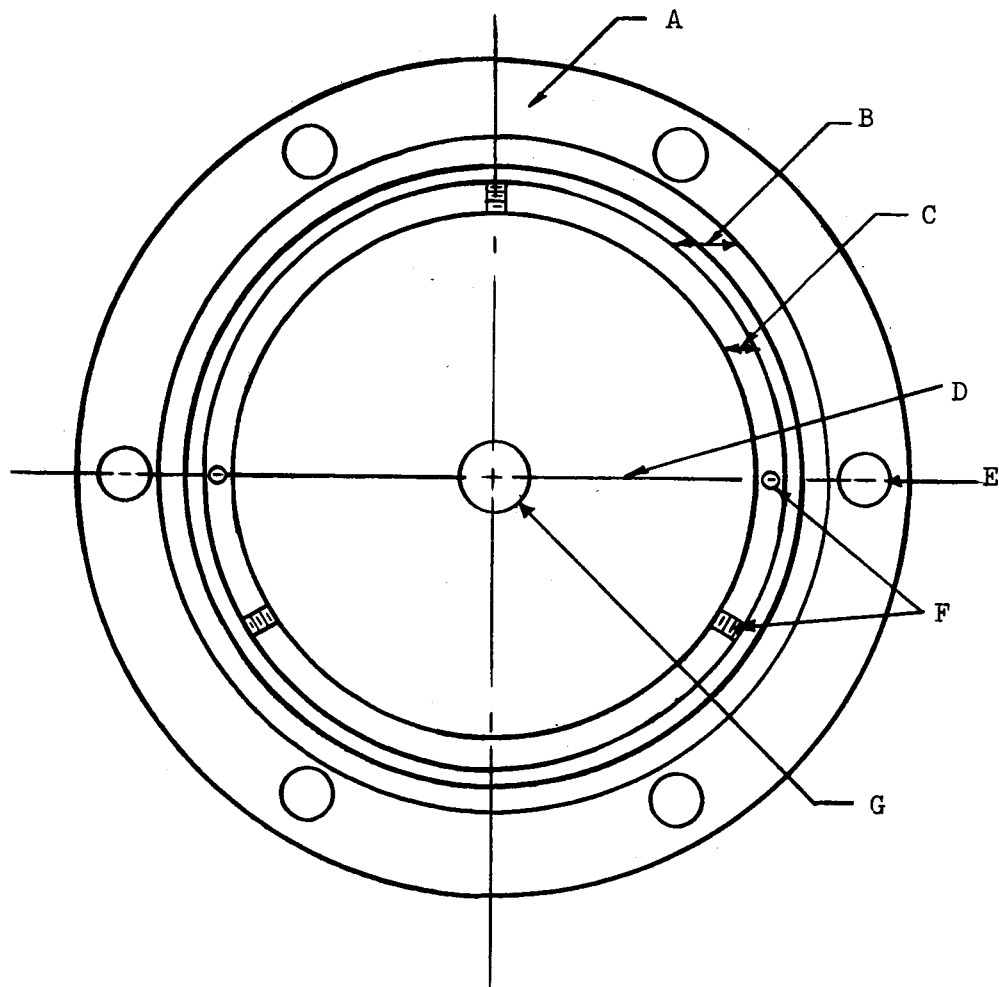
C - WIRE SUPPORT   G - BEAM

D - PIVOT WIRE

FIGURE 4   BEAM SUPPORT

passed 0.050 in. copper electrical leads to the molybdenum sample holders

(B). The sample holders were carefully insulated with a high temperature

ceramic cement. All electrical leads were shielded with alumina tubing

and ceramic cement.

The iron slug (L_1), Figure 3, was fixed to the end of the torsion

beam and was used in conjunction with an external permanent magnet (M) to

fix the relative position of the samples. The strain gauge (N) mounted on

the torsion beam supported a second iron slug (L_2) which interacted with

the field of a solenoid (O). Thus, as current in the solenoid was in-

creased, the samples were moved into contact and loaded normally. The

force of shearing the magnetic flux between the iron slug (L_1) and the

magnet (M) before contact, and the loading force after contact, were mea-

sured by the 0.00095" x 6" nude constantan wire strain gauge. The strain

gauge output was monitored by a Sanborn Transducer-Amplifier, Model 312.

Following each run, the balance system was calibrated in air throughout

the range of operation, i.e. 0 - 7.5 gm, and was found to have a sensi-

tivity of about ± 0.010 gm.

The contact resistance between the samples was measured with a

Leeds and Northrup Precision Kelvin bridge in conjunction with a Keithley

Nanovoltmeter used as a null defector. A Kelvin bridge is designed to

eliminate the effects of lead and contact resistances. It is therefore

useful in measuring very small resistances (when lead and contact re-

sistances become significant). With the Kelvin bridge, it is necessary

to have four leads to the unknown resistance; two are called current

leads and the other two are called potential leads.

Figure 5 is a schematic of the Kelvin bridge circuit. The voltage

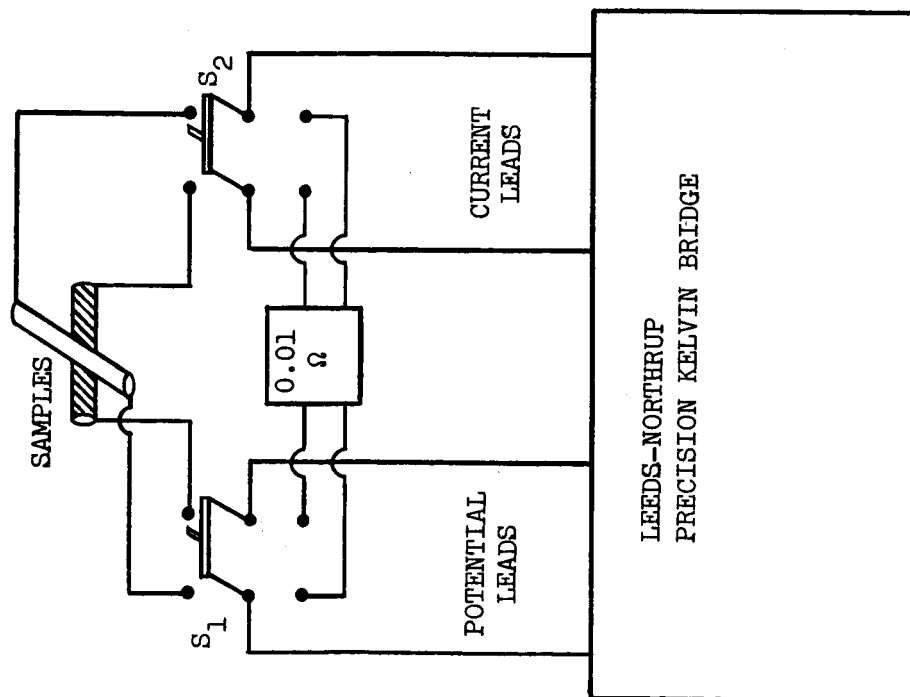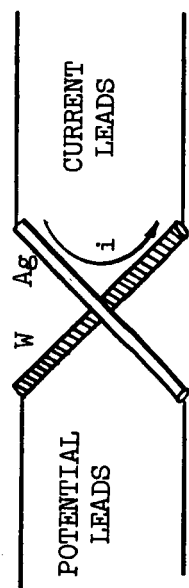source maintained a potential drop of 0.3 millivolts across the contact

CURRENT
LEADS

W Ag

i

POTENTIAL
LEADS

FIGURE 6 LEADS TO CONTACT AREA

S_2

SAMPLES

0.01
Ω

CURRENT
LEADS

POTENTIAL
LEADS

S_1

LEEDS-NORTHRUP
PRECISION KELVIN BRIDGE

FIGURE 5 KELVIN BRIDGE

resistance, which should yield negligible temperature rise at the contact region due to current flow (24). Prior to each run, the bridge was calibrated using a 0.01 ohm NBS standard resistor. Then, using switches S_1 and S_2, the standard resistor was isolated, and the samples were incorporated in the circuit. Figure 6 shows the details of the current and potential connections to the samples. With this configuration, the samples themselves are used as leads to the contact region, and the only resistance measured is the actual contact resistance. This enabled the contact resistance to be measured with an accuracy of 3-4 figures.

The torsion beam arrangement was designed in order to obtain, as nearly as possible, pure normal loading. In this way, shear deformation of the adhesion specimens was reduced to a minimum during test cycles, the only tangential motions coming from unavoidable, normal laboratory vibrations. The effects of these vibrations could be observed only under extremely light specimen loading (< 30 mg) or non-adhesion conditions, when instability of the contact resistance occurred.

The normal operating procedure involved placing the samples in the system and evacuating to a pressure below 10^{-5} Torr, at which time the bakeout cycle started, as previously mentioned, to attain an ultimate pressure of about 2×10^{-10} Torr. The specimens were then subjected to argon ion bombardment for about 5 minutes to remove any gross impurities that may have been adsorbed on the surfaces during bakeout. (If degassing was started immediately, it is possible that these impurities could diffuse into the bulk and later could provide a source of contamination for the surfaces.) Ultra-high purity argon, obtained from the Airco Company, was admitted to the leak system by breaking the capsule break-off tip. The argon was then admitted to the cell to a pressure of about 10^{-4} Torr, and

bombardment was obtained by placing a D.C. potential of about one kilovolt between the filament (D), Figure 3, and the surface to be cleaned. During the entire cleaning operation, a small nickel shield was placed between the samples to shield the sample not being cleaned at that time from contamination.

After about 5 minutes, the bombardment was stopped and the argon evacuated. The cleaning of the tungsten sample was accomplished in several stages:

(1) Resistance heating to about 1800°K in 10^{-6} Torr oxygen for about 15 minutes to permit the carbon on the tungsten surface to be oxidized to form carbon monoxide which could then be evacuated.

(2) Heating by electron bombardment from filament (D) to about 2000°K for at least 12 hours, finally attaining a pressure $< 10^{-9}$ Torr at temperature.

(3) Repeated flashing to 2400°K by resistance heating for a few seconds, to a total of about 15 minutes at 2400°K at a pressure of $< 10^{-9}$ Torr.

The silver was heated by electron bombardment to about 1100°K for one hour. A momentary pressure peak of about 10^{-7} Torr was observed, which fell within a few seconds to below 10^{-9} Torr. While the silver was still hot, the tungsten was again flashed several times to about 2400°K to remove gases adsorbed on the surface during the outgassing of the silver.

Argon ion bombardment was again initiated. At this stage, each surface was bombarded for at least three hours. After bombardment, a substantial deposit of sputtered material was observed on the cell walls

indicating that a considerable amount of surface material was removed.

After this phase, both samples were annealed for an hour to minimize surface damage and to desorb argon from the sample. The tungsten was held at about 2000°K, and the silver at about 1100°K during annealing.

Adhesion cycles were performed at each stage of surface cleanliness, i.e. in air, after bakeout, after degassing and argon bombardment, and after annealing. In the fully clean state, the tungsten was flashed to 2400°K and the silver was heated to 1100°K every hour when measurements were being made.

An adhesion cycle was performed by slowly bringing the samples into contact by increasing the current in the solenoid in discrete intervals. The value of the load on the beam as detected by the Sandborn-312 was noted at each interval until sample contact was made. After contact, contact resistance as well as load was measured for each new adjustment of solenoid current. The loading continued to some predetermined level and was then reduced by increments until contact was broken. Contact make and break were immediately indicated by a closed and open circuit in the Kelvin bridge.

Adhesion was indicated by a greater load on the beam at contact make than at contact break. This can be seen by considering the moments acting on the beam during the cycle (Figure 7). On loading, just before contact, there is a counterclockwise moment M_1 due to the force F_1 from the positioning magnet, and a clockwise moment M_2 due to the loading force F_2 from the solenoid. Now assume that the couple has been loaded, that a force of adhesion F_A has been established, and that the couple is now being unloaded. From Figure 5 it is evident that the moment due to F_A, M_A, is clockwise (as is M_2). Thus, there is a greater total clockwise
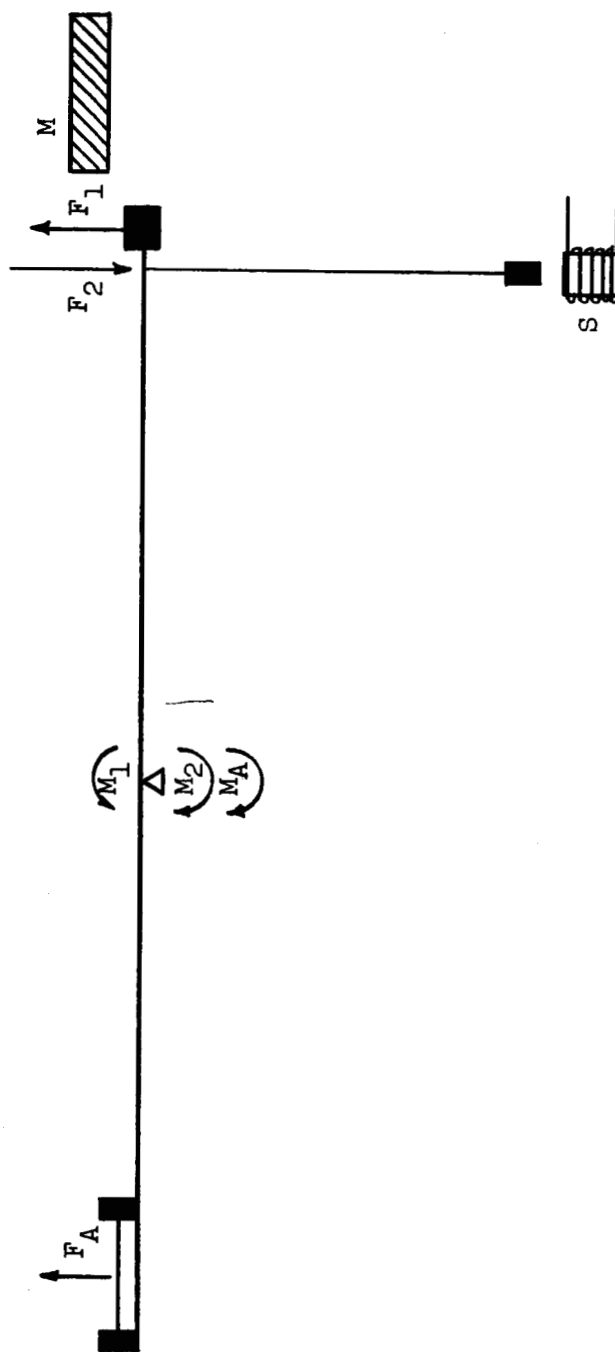
FIGURE 7   MOMENTS AND FORCES ON BEAM.

moment to oppose the effects of M_1. Therefore, M_2 (or equivalently F_2) can fall to a lower value at contact break than at contact make.

In all, a total of about 250 adhesion tests were performed during 8 different runs. As previously mentioned, tests were made for each state of surface cleanliness; also, the peak load on the couple was varied, usually including 0.5, 1.0, 3.0 and 6.0 gm.

In this study, the materials used were:

      (1)   99.999% Ag (0.040" wire)

      (2)   99.99% W (0.030" wire)

both obtained from the United Mineral and Chemical Corporation.

RESULTS AND DISCUSSION

The results of typical adhesion test cycles are shown in Figures 8a and 8b, in which contact resistance is plotted vs load on the couple. Adhesion was observed in the cycle represented in Figure 8a and no adhesion was observed for the cycle in Figure 8b.

Three criteria for metallic adhesion have been established (2) and are evident in Figure 8a:

(1) There is a significant difference between the contact make load and the contact break load.

(2) The minimum contact resistance attained at maximum load on the couple is maintained on unloading to, or very near to, the point of junction fracture.

(3) The contact resistance values are quite stable, even under light loading.

No adhesion was observed in the cycle represented in Figure 8b and, as is evident, each of the three criteria is violated.

(1) There is no significant difference between contact make force and contact break force.

(2) Minimum contact resistance is not maintained on unloading; indeed, there is little or no difference between the loading and unloading branches of the contact resistance-load curve.

(3) For light loads, the contact resistance values are unstable.

250 adhesion test curves were obtained for various stages of surface cleanliness, and various loads on the couple. The results for the various stages may be summarized as follows:

Stage (1) - In air, the minimum contact resistance averaged about 1 ohm, and no adhesion was ever observed.
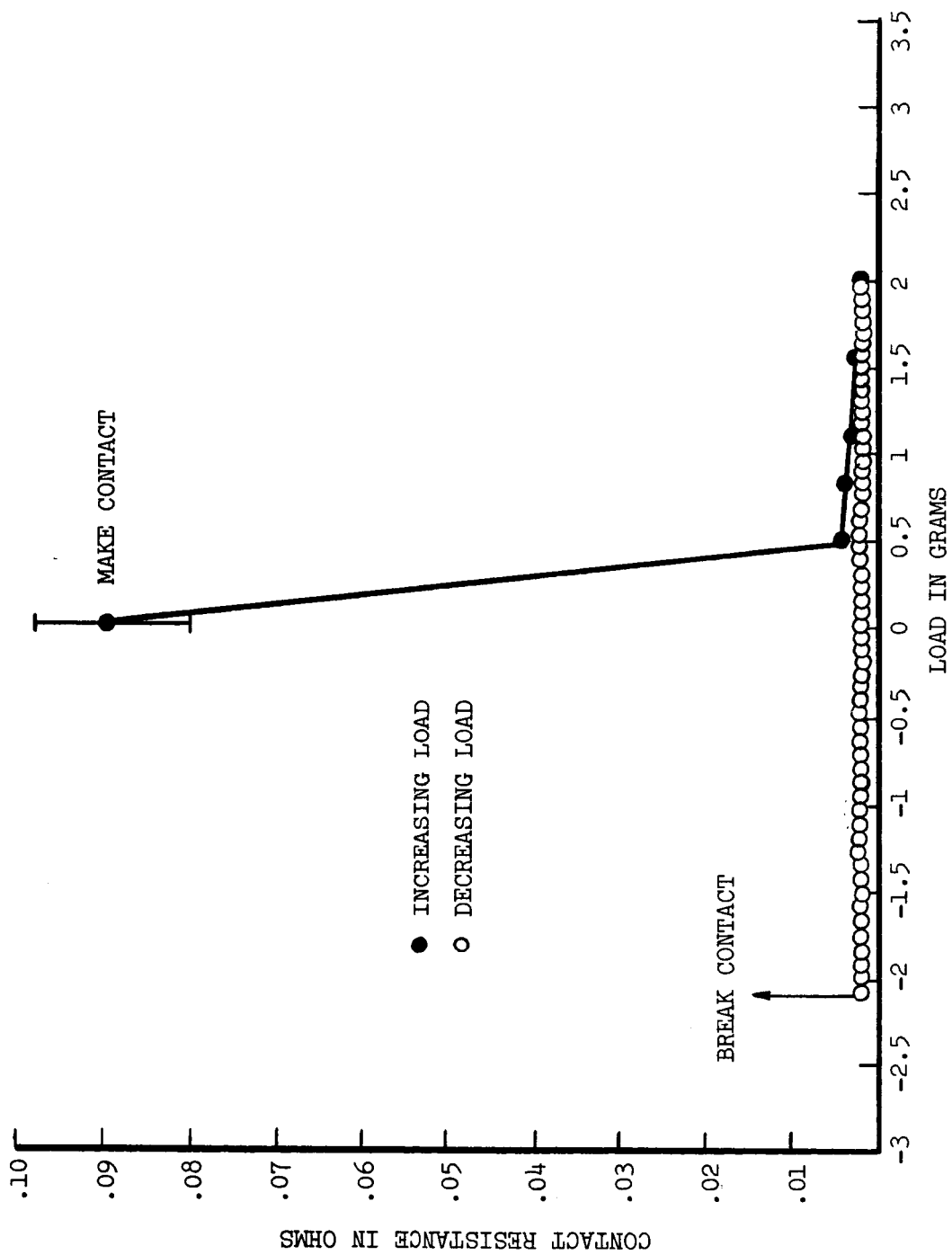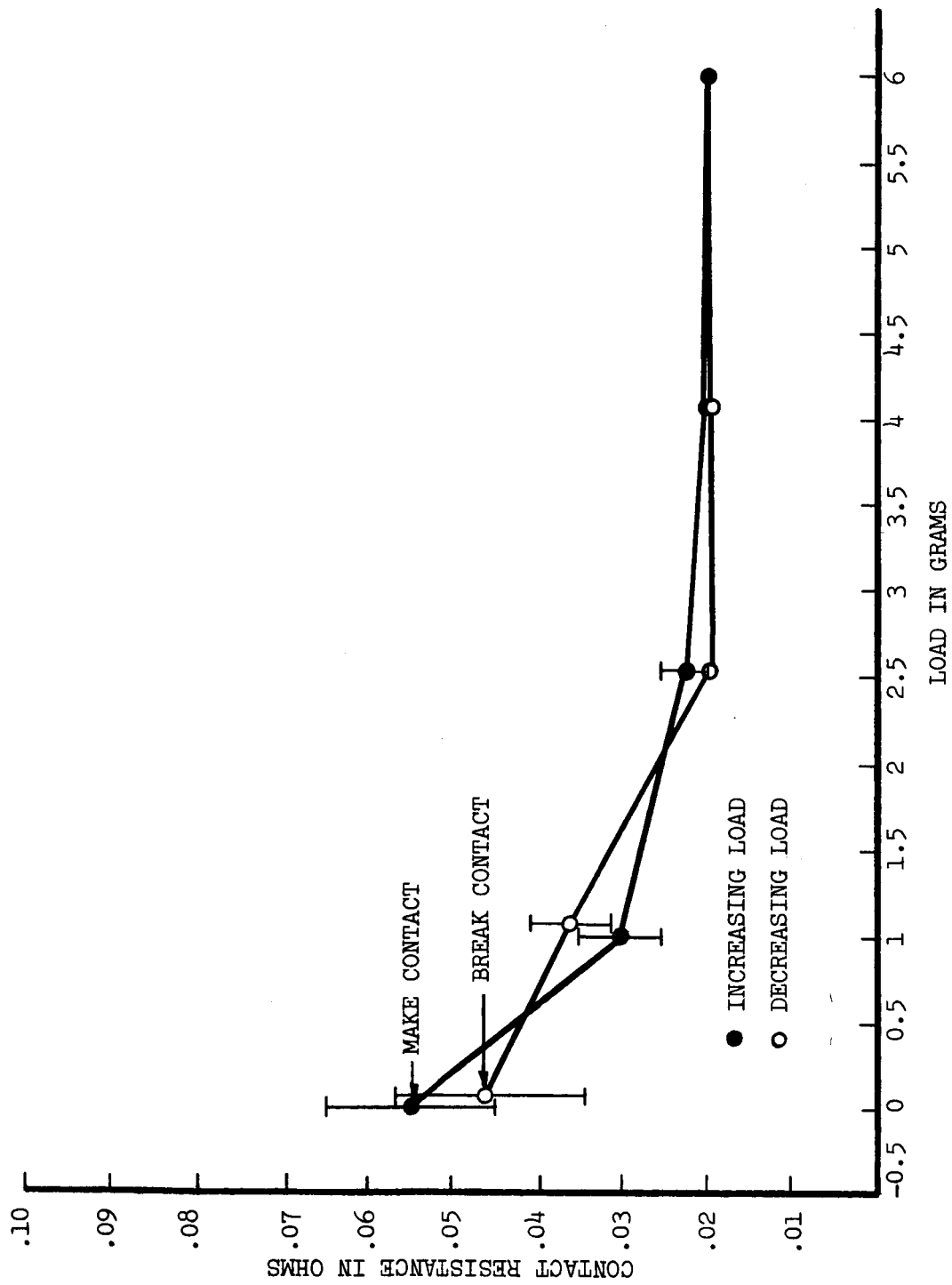
FIGURE 8a ADHESION CYCLE, ADHESION ACHIEVED.

FIGURE 8b   ADHESION CYCLE, NO ADHESION.

Stage (2) - Samples tested at ambient pressures of 10^{-6} Torr and before bakeout gave results which were identical to those in air.

Stage (3) - After bakeout and degassing of auxiliary components, i.e. not the samples, (pressure about 2 x 10^{-10} Torr) the average minimum contact resistance was about 0.08 ohm, and adhesion was still not observed.

Stage (4) - The silver was degassed and argon ion bombarded and the tungsten heated in oxygen to 1800°K, annealed at 2000°K and argon bombarded, but not flashed to 2400°K. After this treatment the average minimum contact resistance fell to about 0.02 ohm, and adhesion was found in roughly 10% of the cycles. Identical results were found for measurements in about 10^{-4} Torr argon, and for measurements after the argon had been pumped off, leaving the system about 2 x 10^{-10} Torr.

Stage (5) - The silver was annealed, and the tungsten flashed to 2400°K repeatedly. At this stage, minimum contact resistance fell to about .002 ohms, and strong adhesion was noted in about 90% of all cycles

Stage (6) - When the fully clean surfaces were deliberately contaminated with several monolayers of oxygen, the contact resistance rose to about .01 ohms, and no adhesion was observed.

These results are also summarized in Figure 9. The curves are envelopes which contain all of the adhesion cycles for Stages 3, 4 and 5. The significant points are that as surface cleanliness increases, contact resistance decreases and contact resistance scatter decreases, as indicated by the narrowing of the envelopes.

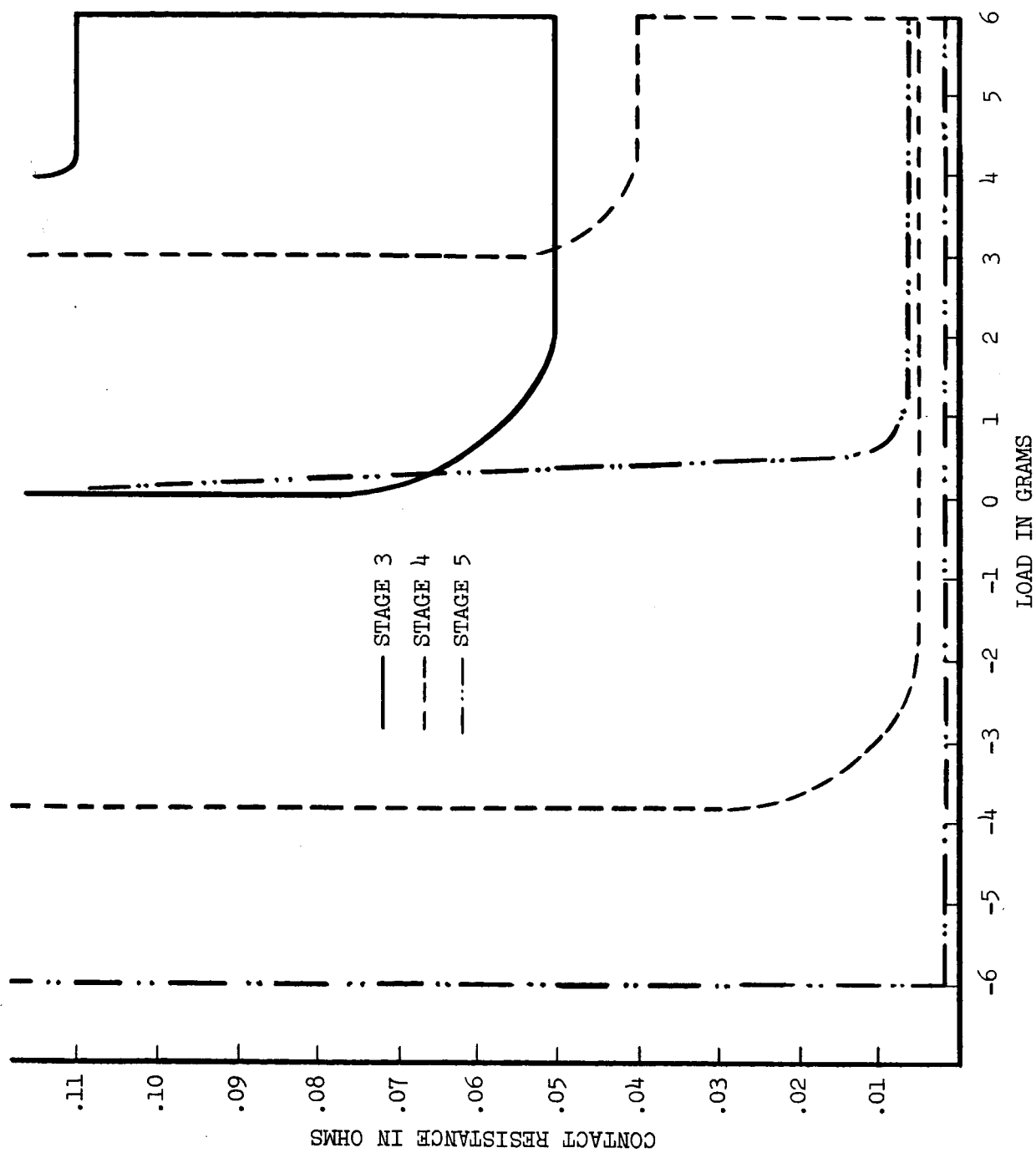The envelopes of the adhesion cycles for Stages 3, 4 and 5 are

FIGURE 9   CYCLE ENVELOPES FOR STAGES 3, 4, AND 5.

presented in Figures 10, 11 and 12. The cross-hatched areas within these curves represent the envelopes containing 80% of all the pertinent adhesion cycles. These "80% envelopes" illustrate how dramatic the decrease in scatter and increase in the incidence of adhesion was from Stage 3 to Stage 5. They are presented side by side in Figure 13. The decrease in scatter and the drop in contact resistance implies that in Stage 3, the surfaces were thoroughly contaminated, and that the degree of contamination varied greatly over the surface. In Stage 4, both surfaces were probably lightly contaminated over most of the surfaces, although there were still spots that were more heavily contaminated. It is felt that in Stage 5, the surfaces were atomically clean except for a few spots of light contamination. This, of course, cannot be proved but in other investigations, similar cleaning techniques have yielded atomically clean surfaces for tungsten (25,26) and silver (27). Figure 14 summarizes the observations of the effect of surface cleanliness on contact resistance and adhesion. When the surfaces were badly contaminated, adhesion was never observed even for high loads. For clean surfaces, adhesion was observed for loads < 0.5 gm. It is therefore concluded that contamination was the major barrier to adhesion.

If the Hertz equation is used to calculate $\underline{a}$, the radius of the contact area, and this is substituted into Holm's equation for the contact resistance,

$$R_c = \frac{\rho_{Ag}}{4a} + \frac{\rho_w}{4a} \qquad (4)$$

an estimate of the contact resistance for an atomically clean junction is obtained. For a load of 1.5 gm, this method of estimation gives a contact resistance of about 5×10^{-3} ohms. Experimentally, a value of 2×10^{-3} ohms was obtained. Thus, the observed contact resistance does not seem
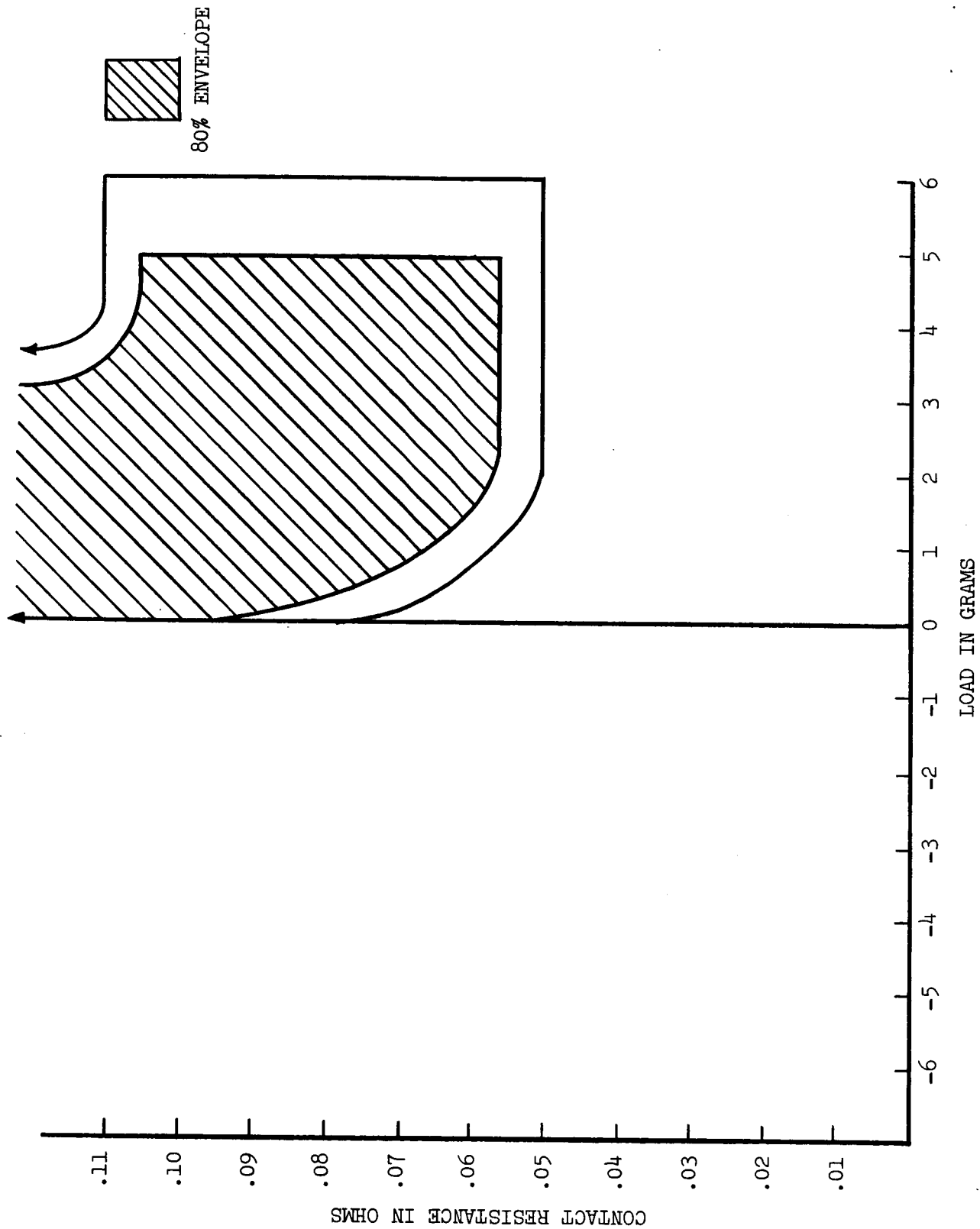
FIGURE 10   CYCLE ENVELOPE FOR STAGE 3.

80% ENVELOPE

LOAD IN GRAMS
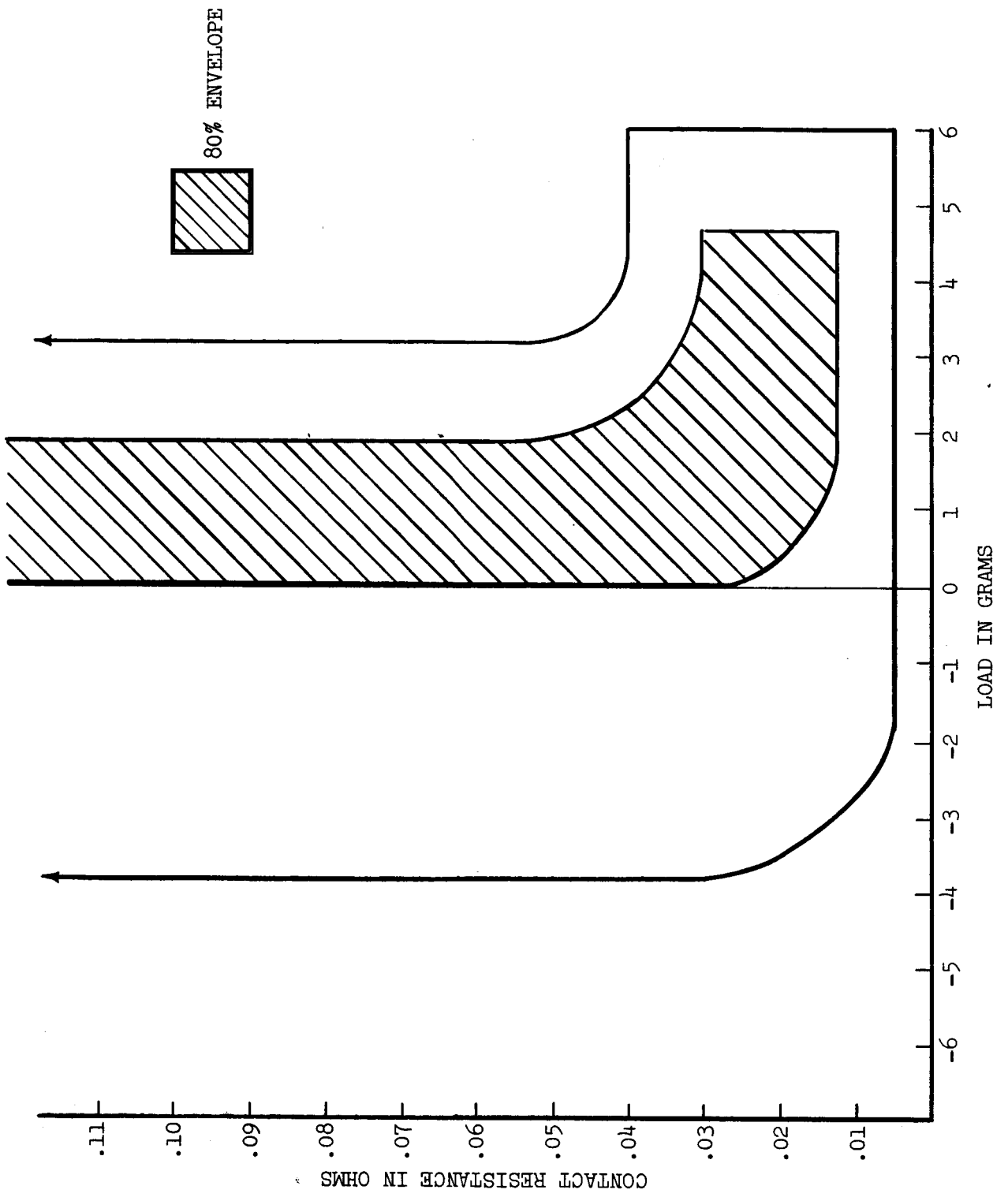
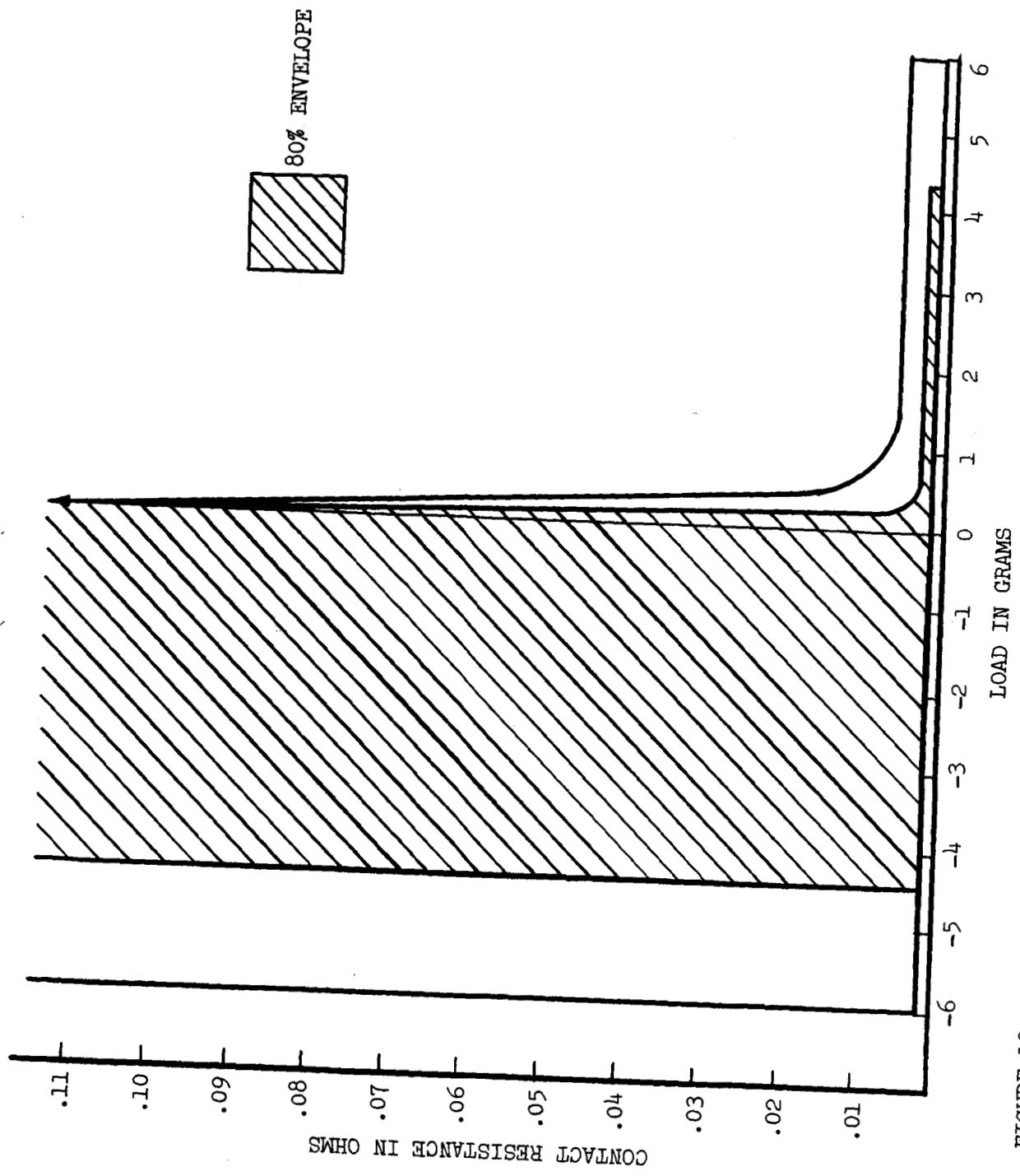CONTACT RESISTANCE IN OHMS

FIGURE 11   CYCLE ENVELOPE FOR STAGE 4.

FIGURE 12 CYCLE ENVELOPE FOR STAGE 5.

80% ENVELOPES

LOAD IN GRAMS

CONTACT RESISTANCE IN OHMS

STAGE 3
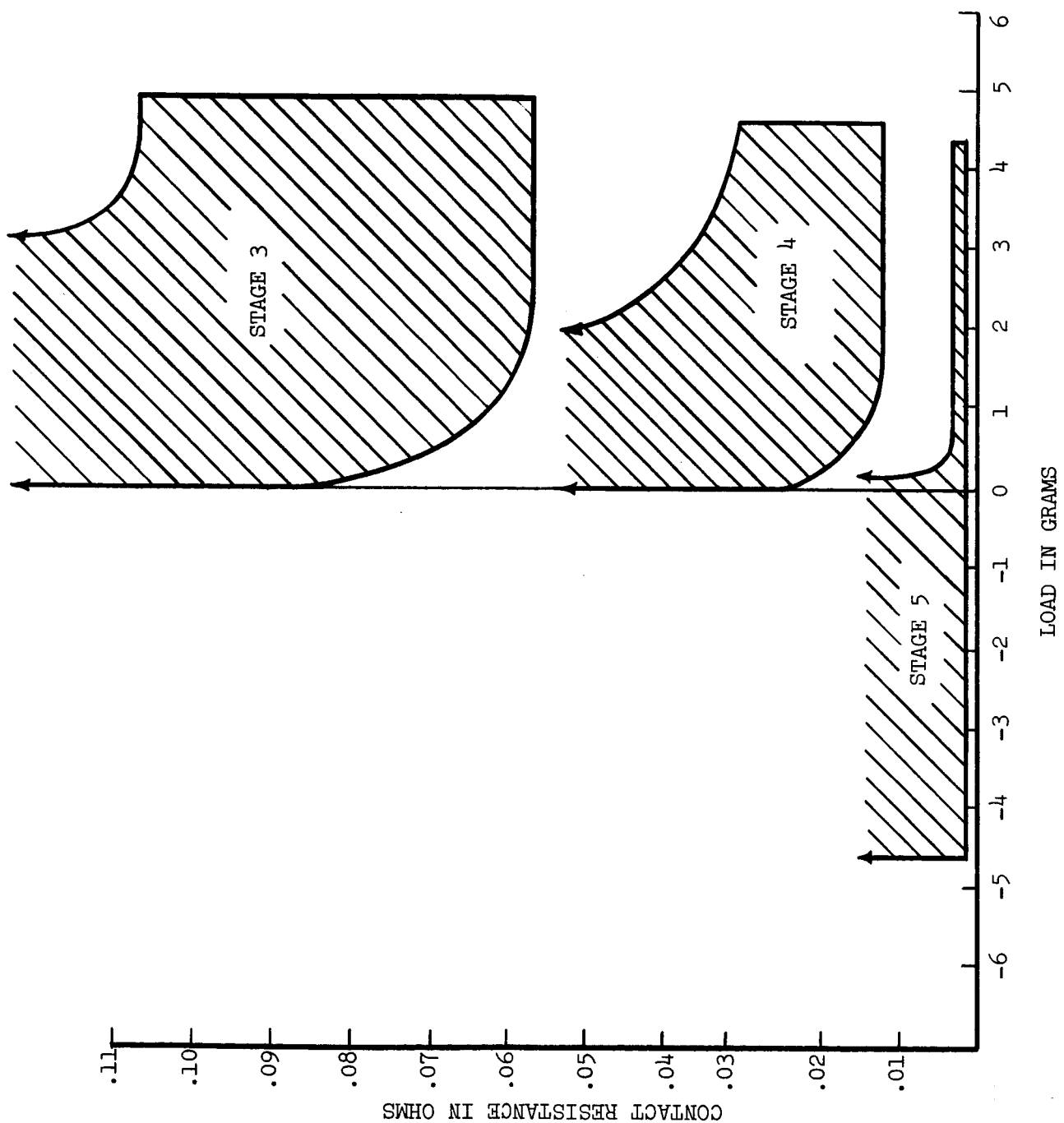
STAGE 4

STAGE 5

FIGURE 13   80% ENVELOPES FOR STAGES 3, 4, AND 5.

CONTACT RESISTANCE IN OHMS

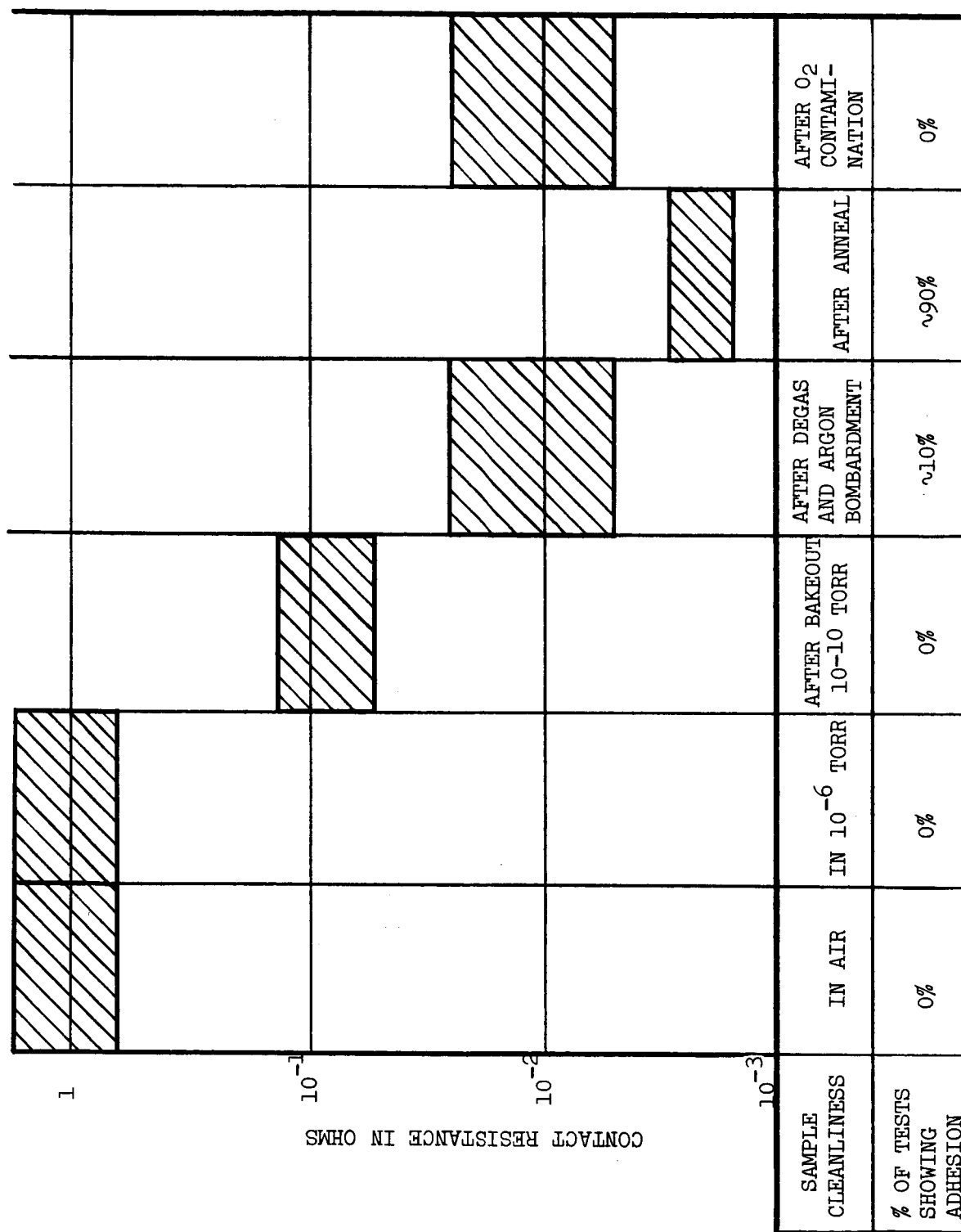| SAMPLE CLEANLINESS	IN AIR	IN 10^{-6} TORR	AFTER BAKEOUT 10-10 TORR	AFTER DEGAS AND ARGON BOMBARDMENT	AFTER ANNEAL	AFTER O_2 CONTAMINATION
% OF TESTS SHOWING ADHESION	0%	0%	0%	~10%	~90%	0%

FIGURE 14 CONTACT RESISTANCE VS. SURFACE CLEANLINESS

anomalously high, which is in contrast to the high values reported by

Johnson and Keller (1) for the copper-nickel and silver-nickel couples.

It is interesting to compare the observed contact resistance to that

reported by Johnson and Keller for silver-silver. A load of 0.78 gm for a

silver-silver couple gives the same contact area as a load of 1.5 gm on a

silver-tungsten couple according to the Hertz formula. For this load,

the silver-silver contact resistance was found to be about 2×10^{-3} ohms.

This suggests that R_c for atomically clean surfaces may be strongly de-

pendent upon contact area, and only weakly dependent upon the resistivities

of the materials involved. This is not what would be expected if Equation

(4) is valid. Equation (4) cannot be refuted by this rather weak evidence,

but there is now sufficient doubt in its validity to suggest that further

research in this area would be very interesting.

Figure 15 is a plot of joint strength vs load on the couple for the

fully clean state. As mentioned in the Theory Section, for loads less than

1.5 gm, the Hertz elastic formula should be valid, and for greater loads

the Holm contact resistance formula should be valid. It was found, how-

ever, that Holm's formula gave reasonable values for all loads, while

Hertz' formula could only be applied for loads less than 1.5 gm. In any

case, the important feature of Figure 13 is the absence of any relation

between the load on an adhesion couple and its adhesion strength. This is

in agreement with the previous observations of Johnson and Keller (2,12).

It should also be noted that the tensile strengths of the couples are close

to the tensile strength of annealed silver. The scatter in the joint

strength may be due to localized surface contamination, variations in

surface geometry (asperities), and work hardening of the silver.

In this investigation, adhesion strengths approximating the tensile
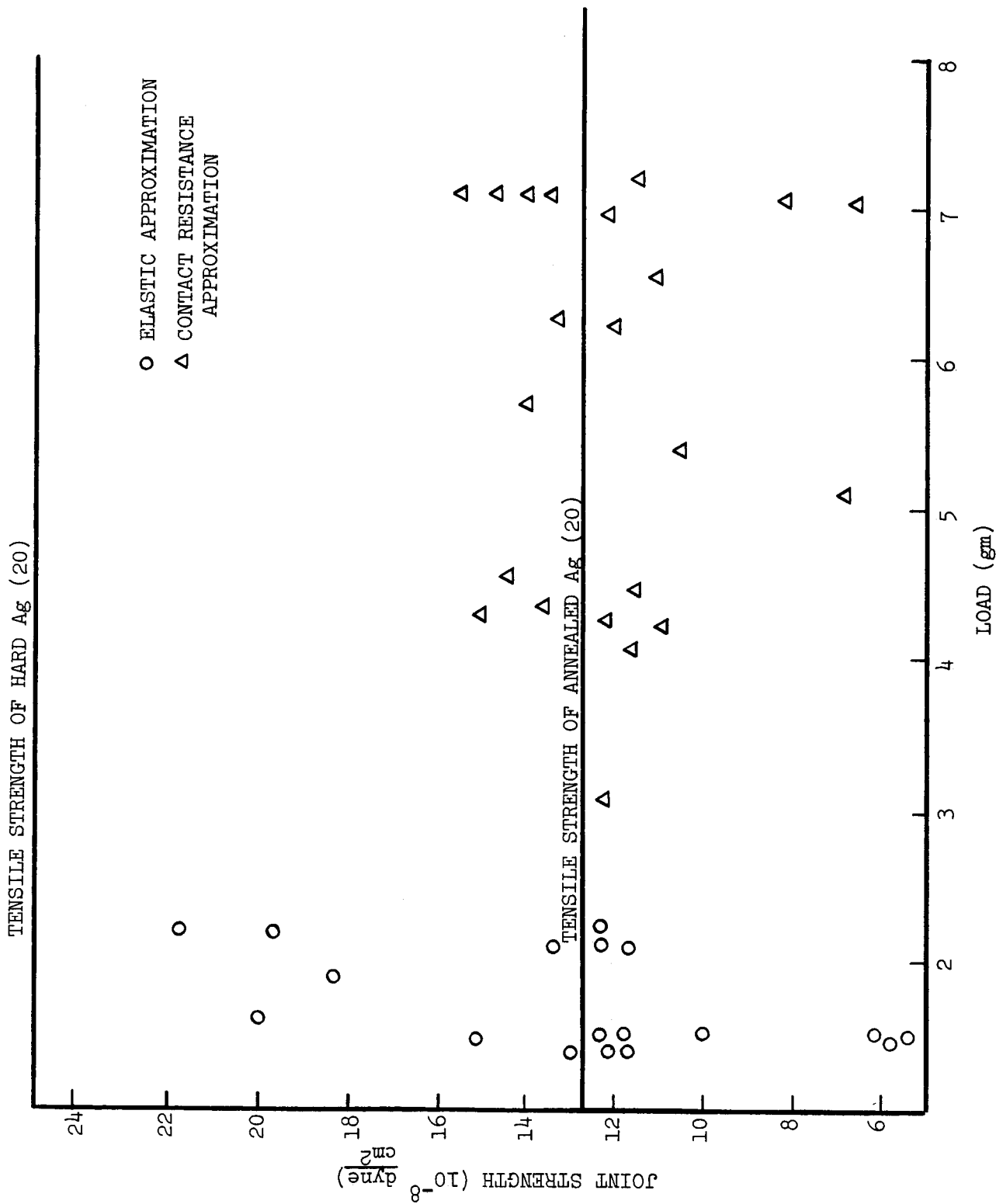
FIGURE 15 JOINT STRENGTH VS. LOAD.

strength of the weaker metal have been observed for the insoluble metals, tungsten and silver. This is consistent with the observations of Johnson et al for Ag-Ag, Ag-Ni, Cu-Ni, Mo-Mo and Ti-Ti. Since strong adhesion has now been observed for two immiscible systems using the method of Johnson et al, i.e. Ag-Ni and Ag-W, it seems doubtful that bulk miscibility is a criterion for metallic adhesion, as previously suggested.

Intuitively, bulk miscibility would seem to be a very logical criterion for adhesion. One could imagine an interface between the two immiscible solid metals, across which there could be no diffusion of the metals into each other. Such a system would be expected to fracture more readily in tension than a system in which the metals could diffuse into each other, forming an interface of finite thickness and varying concentration. Such a model is apparently not valid since strong adhesion between immiscible metals was, in fact, observed. However, an error is exposed when the model is carefully examined. When corrected, the model satisfactorily explains adhesion between immiscible metals. The error lies in the assumption that the characteristics of the bulk metals can be used to explain adhesion, which is primarily a _surface_ phenomenon. Many investigations have shown that surface phenomena are often unrelated to bulk phenomena (28,29). It is generally accepted, for example, that in the solid-vacuum interfaces of diamond (30), silicon (31) and germanium (31), the diamond type lattice of the bulk is replaced by a hexagonal structure. This region is thought to be of the order of 5 atomic layers deep.

Hudson (32) has observed and measured a finite binding energy of cadmium to a tungsten substrate in a mass spectrographic investigation. These metals are mutually insoluble in the bulk.

The work of Taylor (33) on the immiscible system, copper-tungsten, is of particular significance. In a low energy electron diffraction study of the epitaxy of copper films on atomically clean surfaces of tungsten, he found that the copper penetrated the tungsten to a depth of about 5 atomic layers. It is probable that a similar phenomenon occurs in the Ag-W system; perhaps it occurs in all bulk immiscible systems.

Cahn and Hilliard (34), in a thermodynamic analysis of interface systems, used a model in which the interface was considered to be of finite thickness with a concentration gradient across this thickness. The thickness of the interface was shown to depend on the interaction energies of the atomic species involved and the reduced temperature (absolute temperature/absolute critical temperature). The critical temperature is the temperature at which the two materials will interpenetrate by diffusion to permit the formation of an equilibrium solution.

If the Cahn and Hilliard model is applicable, every pair of miscible metals in physical contact at any temperature above absolute zero will have an interfacial region of varying composition, with a finite thickness dependent on the critical temperature for that system. Since the composition varies across the interface, the tensile strength also varies across the interface, and is likely to be minimum at one of the boundaries of the interface, i.e. in the weaker of the two pure metals.

Thus, if we accept the postulate that metals that are immiscible in the bulk are miscible in the first few atomic layers, the above diffuse interface model for metallic adhesion is consistent with the experimental results of Johnson and Keller (2,12) and this investigation. It predicts that all metallic couples with clean surfaces will adhere, and that the strength of the cold-welded couple will be the strength of the weaker member.

CONCLUSIONS AND RECOMMENDATIONS

(1) Metallic adhesion was observed for the silver-tungsten system, and
     was comparable to that observed by Johnson and Keller for the
     silver-silver, silver-nickel, molybdenum-molybdenum and titanium-
     titanium systems.

(2) Contamination was found to be the major barrier to adhesion in the
     system.

(3) Deliberate contamination of atomically clean samples with several
     monolayers of oxygen prevented adhesion, and raised the contact
     resistance from about 2×10^{-3} ohms to 10^{-2} ohms.

(4) Immiscibility was found to be no barrier to silver-tungsten adhesion
     which is consistent with recent observations that bulk immiscible
     metals may be miscible in the first few atomic layers. From this,
     and the Cahn-Hilliard model of an interface, a model for metallic
     adhesion was suggested.

(5) The contact resistance values found for the fully clean state were
     close to those expected theoretically. However, a number of
     anomalies in the area of contact resistance between dissimilar
     metals were pointed out, and it was suggested that further study
     is needed in this area.

(6) It is recommended that further work be done on true contact area
     measurements, since an accurate method of measuring contact area
     would probably eliminate much of the scatter in joint strengths
     found in this study.

(7) The Cahn-Hilliard model of an interface predicts a variation of
     interface thickness with temperature. A study of the variation in
     the adhesion force from cryogenic temperatures to high temperatures

would be very useful in establishing the validity of the proposed model for adhesion.

(8) Further studies of the interdiffusion of bulk immiscible metals would also be useful.

REFERENCES

(1)   D.V. Keller, Jr., "Physical and Chemical Characteristicis of Surfaces and Interfaces, Syracuse University Press, to be Published (1967).

(2)   K.I. Johnson, and D.V. Keller, Jr., J. Appl. Phys. $\underline{38}$, 1896 (1967).

(3)   D.R. Milner, and G.W. Rowe, Met. Rev., $\underline{7}$, No. 28, 433 (1962).

(4)   M.E. Sikorski, "Mechanisms of Solid Friction, eds. P.J. Bryant, M. Lavik and G. Solomon, Elsevier Pub. Co., Amsterdam (1964).

(5)   A.P. Semenov, Wear, $\underline{4}$, 1 (1961).

(6)   W.P. Gilbreath, ASTM-ASLE Symposium on the Adhesion of Materials in Space Environments, Toronto (1967).

(7)   H. Conrad and L. Rice, ASTM-ASLE Symposium, ibid.

(8)   T.H. Batzer, and R.F. Bunshah, J. Vac. Sci.,$\underline{4}$, 19 (1967).

(9)   J.L. Ham, ASLE Transactions $\underline{6}$, 20 (1963).

(10) M.J. Hordon, ASTM-ASLE Symposium on the Adhesion of Materials in Space Environments, Toronto (1967).

(11) D.V. Keller, Jr., Wear, $\underline{6}$, 353 (1963).

(12) K.I. Johnson and D.V. Keller, Jr., J. Vac. Sci., $\underline{4}$, 115 (1967).

(13) D.V. Keller, Jr., and T. Spalvins, Trans. Vac. Met. Cont., ed. R.F. Bunshah, Amer. Vac. Soc. Pub. 149, Boston (1963).

(14) F. Erdmann-Jesnitzer, Aluminum, $\underline{33}$, 730 (1957).

(15) A.P. Semenov, Wear, $\underline{4}$, 1 (1961).

(16) F.P. Bowden, and G.W. Rowe, Proc. Roy. Soc., $\underline{233a}$, 429 (1955).

(17) F.P. Bowden, and D. Tabor,"The Friction and Lubrication of Solids, Part II", Clarendon Press, Oxford, England (1964).

(18) R. Holm, Electric Contacts Handbook, Springer-Vertag, Berlin, Germany (1958).

(19) J.A. Greenwood, Burndy Research Division, Report No. 38 (1966).

(20) D. Tabor, "The Hardness of Metals", Clarendon Press, Oxford, England (1951).

(21) H. Hertz, see S. Timoshenko and J.N. Goodier, "Theory of Elasticity", McGraw-Hill (1951).

REFERENCES (Cont'd.)

(22) Metals Handbook, American Society for Metals, Cleveland, Ohio (1948).

(23) K.I. Johnson, and D.V. Keller, Jr., Syracuse University Research Institute, Report Met. 1311-63066 (1966).

(24) J.B.P. Williamson, Proc. Inst. Elec. Eng., 109A, 224 (1962).

(25) H.D. Hagstrum, and C. D'Amico, J. Appl. Phys., 31 (1960).

(26) J.A. Becker, E.J. Becker, and R.G. Brandes, J. Appl. Phys., 32 (1961).

(27) H.E. Farnsworth in "The Surface Chemistry of Metals and Semiconductors", H.C. Gatos, ed., Wiley, New York (1960).

(28) J.C. Ericksson, "Advances in Chemical Physics VI, Interscience, New York (1964).

(29) P.L. de Bruyn, in Fundamental Phenomena in Natural Sciences, Phenum Press, New York (1966).

(30) H.E. Farnsworth, and J.B. March in International Conference on Physics of Semiconductors, Institute of Physics, publisher, London (1962).

(31) J.J. Lander, and J. Morrison, J. Appl. Phys., 34, 1403 (1963).

(32) J.B. Hudson, private communication (1967).

(33) N.J. Taylor, Surface Science, 4, 161 (1966).

(34) J.W. Cahn, and J.E. Hilliard, J. Chem. Phys., 28, 258 (1958).